



# Observed changes in brown, white, hepatic and pancreatic fat after bariatric surgery: Evaluation with MRI

Steve C. N. Hui<sup>1</sup> · Simon K. H. Wong<sup>2</sup> · Qiyong Ai<sup>1</sup> · David K. W. Yeung<sup>1,3</sup> · Enders K. W. Ng<sup>2</sup> · Winnie C. W. Chu<sup>1</sup>

Received: 16 March 2018 / Revised: 29 May 2018 / Accepted: 15 June 2018 / Published online: 30 July 2018  
© European Society of Radiology 2018

## Abstract

**Objectives** To study the change in brown and white adipose tissue (BAT and WAT), as well as fat content in the liver and pancreas, in patients with morbid obesity before and after bariatric surgery.

**Methods** Twelve patients with morbid obesity (F=8, M=4, age: 45.4 years (38.4–51.2), BMI: 35.2 kg/m<sup>2</sup> (32.5–38.6)) underwent pre-op MRI at baseline and two post-op scans at 6-month and 12-month intervals after bariatric surgery. Co-registered water, fat, fat-fraction and T2\* image series were acquired. Supraclavicular BAT and abdominal WAT were measured using in-house algorithms. Intrahepatic triglyceride (IHTG) was measured using MR spectroscopy and pancreatic fat was measured using a region-of-interest approach. Fat contents were compared between baseline and the first and second 6-month intervals using non-parametric analysis of Friedman's test and Wilcoxon's signed-rank test. Level of significance was selected at  $p=0.017$  (0.05/3). Threshold of non-alcoholic fatty liver disease was set at 5.56%.

**Results** Results indicated that BMI ( $p=0.005$ ), IHTG ( $p=0.005$ ), and subcutaneous ( $p=0.005$ ) and visceral adipose tissues ( $p=0.005$ ) were significantly reduced 6 months after surgery. Pancreatic fat ( $p=0.009$ ) was significantly reduced at 12 months. Most reduction became stable between the 6-month and 12-month interval. No significant difference was observed in BAT volume, fat-fraction and T2\* values.

**Conclusion** The results of this study suggest that bariatric surgery effectively reduced weight, mainly as a result of the reduction of abdominal WAT. Liver and pancreatic fat were decreased below the threshold possibly due to the reduction of free fatty acid. BAT volume, fat-fraction and T2\* showed no significant changes, probably because surgery itself might not have altered the metabolic profile of the patients.

## Key Points

- No significant changes were observed in fat-fraction, T2\* and volume of brown adipose tissue after bariatric surgery.
- Non-alcoholic fatty liver disease was resolved after surgery.
- Abdominal white fat and liver fat were significantly reduced 6 months after surgery and become stable between 6 and 12 months while pancreatic fat was significantly reduced between 0 and 12 months.

**Keywords** Magnetic resonance imaging · Magnetic resonance spectroscopy · Brown adipose tissue · White adipose tissue · Bariatric surgery

## Abbreviations

BAT	Brown adipose tissue
BMI	Body mass index
ICC	Intraclass correlation coefficient
IHTG	Intrahepatic triglyceride
IQR	Interquartile range
LGCP	Laparoscopic greater curvature plication
LSG	Laparoscopic sleeve gastrectomy
NAFLD	Nonalcoholic fatty liver disease
RYGB	Roux-en-Y gastric bypass
SAT	Subcutaneous adipose tissues
UCP1	Uncoupling protein 1

✉ Winnie C. W. Chu  
winniechu@cuhk.edu.hk

<sup>1</sup> Department of Imaging and Interventional Radiology, Prince of Wales Hospital, The Chinese University of Hong Kong, Sha Tin, New Territories, Hong Kong SAR

<sup>2</sup> Department of Surgery, Prince of Wales Hospital, The Chinese University of Hong Kong, Sha Tin, New Territories, Hong Kong SAR

<sup>3</sup> Department of Clinical Oncology, Prince of Wales Hospital, The Chinese University of Hong Kong, Sha Tin, New Territories, Hong Kong SAR

VAT	Visceral adipose tissues
WAT	White adipose tissue

## Introduction

Obesity is associated with diabetes mellitus type 2, dyslipidemia, hypertension and insulin resistance [1]. It is generally caused by the imbalance in intake and expenditure of energy. Excessive energy is mainly stored in fat cells in the form of white adipose tissue (WAT) in the abdominal region beneath the skin as subcutaneous adipose tissue (SAT) or surrounding the internal organs as visceral adipose tissue (VAT). An imbalance in hepatic fatty acid uptake also causes the accumulation of intrahepatic triglyceride (IHTG), which leads to hepatic steatosis [2]. Brown adipose tissue (BAT) is a special type of lipid that has the capacity to induce thermogenesis [3]. The majority of BAT is located at the supraclavicular fat depot in the interscapular and cervical regions [4]. It was thought to be minimal or that it disappeared after infancy until recent studies re-discovered its existence in adults using FDG PET-CT scans [4, 5]. It is highly specialized for non-shivering thermogenesis due to its unique characteristic of uncoupling protein 1 (UCP1). Activated UCP1 stimulates respiratory chain activity and heat release from the combustion of available substrates [3, 6]. With the ability for heat production and energy regulation, activation of BAT becomes a potential therapy against obesity.

Obesity involves adverse body effects, and many clinical interventions have been proposed to reduce body weight. Research studies have demonstrated promising results on the efficacy of lifestyle modification to achieve weight loss and improve general fitness [7, 8]. Such intensive lifestyle modifications have successfully accomplished the goals during the course of intervention but weight regain commonly occurs years after therapy [9]. Surgical treatment is an alternative option for individuals with severe obesity. Research studies have reported that participants who have undergone bariatric surgery are able to sustain long-term weight loss and show improvements in health perceptions, social interaction and other obesity-related problems [10, 11]. Laparoscopic sleeve gastrectomy (LSG) and laparoscopic Roux-en-Y gastric bypass (RYGB) are common procedures, while greater curvature plication (LGCP) is a relatively recent one [12].

Bariatric surgery is known to be an effective intervention in controlling weight and its efficacy is mainly assessed by the reduction of subcutaneous and visceral adipose tissue, but has rarely been focused on ectopic fat in the liver and pancreas and the metabolically active BAT. The purpose of this study was to measure the change in BAT and WAT at the supraclavicular fat depot, abdominal SAT and VAT, IHTG and pancreatic fat in a group of patients with severe obesity before and after bariatric surgery.

## Materials and methods

The research protocol was approved by the institutional clinical research ethics committee and conducted in compliance with the Declaration of Helsinki. Written informed consent was obtained from all volunteers.

### Selection of participants

Patients with morbid obesity were prospectively recruited from the out-patient clinic at the institutional hospital. Inclusion criteria were patients between the age of 18 and 65 years, BMI  $\geq 30$  kg/m<sup>2</sup> with metabolic syndrome or BMI  $\geq 35$  kg/m<sup>2</sup>, and pending bariatric surgery. Exclusion criteria included weight  $\geq 250$  kg, waist circumference  $\geq 150$  cm and alcohol ingestion of more than 30 g/day for males and 20 g/day for females. The maximum weight and waist circumference were set according to the tolerance of the scanner and the bore size. Baseline MRIs were done before the scheduled surgeries and two post-operative scans were done at 6-month and 12-month intervals. Fourteen participants (female=8, male=4, age: 45.4 years (38.4–51.2), BMI: 35.2 (32.5–38.6)) were recruited to undergo MRI. Twelve of them (seven with co-morbidities of hypertension, dyslipidemia and diabetes and the rest with at least one metabolic condition) successfully completed their surgeries (eight LSG, two RYGB and two LGCP) and two were excluded due to withdrawal from their operations. Ten of them completed MRI at all three time points and two missed their 6-month post-op MRI (M6) scans. Their anthropometries and other MR-based measurements are shown in Table 1.

### Image acquisition

All volunteers underwent MRI using a 3.0 T whole-body scanner (Achieva X-series, Philips Healthcare, Best, The Netherlands) with a 16-channel SENSE-XL-Torso array coil. 3D spoiled chemical-shift water-fat mDixon sequence (TR = 5.7 ms, first TE/echo spacing = 1.2–1.4 (ms)/1.0–1.2 (ms), number of echoes = 6, flip angle = 3°, SENSE acceleration = 2, reconstructed slice thickness/number of slices = 1.5 mm/100 (for the non-breath-hold scan at the upper trunk) and 3.0 mm/50 (for the breath-hold scan at the abdominal region)) was employed to acquire co-registered water, fat, fat-fraction and T2\* image series. Non-breath-hold acquisition was performed from the base of the skull to the base of the thoracic cavity for BAT measurement and breath-hold acquisition was performed from the dome of the diaphragm to the pubic symphysis for abdominal SAT and VAT measurements. Image reconstruction was completed online using Philips mDixon product implementation with the multi-peak spectral model of fat to increase accuracy and sensitivity.

**Table 1** Results of variables measured at different time points

	M0	M6	M12	<i>p</i> -value
Body weight (kg)	96.1 (80.5–103.6)	78.0 (65.2–89.8)	67.9 (61.6–83.0)	<0.001 <sup>†</sup>
BMI (kg/m <sup>2</sup> )	35.2 (32.5–38.6)	27.9 (26.7–32.8)	26.3 (25.4–28.5)	<0.001 <sup>†</sup>
Waist circumference (cm)	111.0 (102.8–122.0)	105.3 (90.5–115.4)	90.5 (84.5–104.0)	<0.001 <sup>†</sup>
Time between surgery and MRI (days)	17.0 (8.25–36.25)	179.0 (154.5–203.5)	371.5 (359.25–431.0)	N/A
Pancreatic fat-fraction (%)	6.71 (4.29–10.57)	5.05 (3.65–6.80)	2.19 (0.68–3.97)	0.027 <sup>†</sup>
Pancreatic T2* (ms)	42.92 (40.52–47.60)	50.86 (45.11–60.57)	51.77 (45.03–69.49)	0.122
Intrahepatic triglyceride (%)	14.66 (3.72–22.35)	2.09 (0.79–3.39)	0.87 (0.24–2.04)	<0.001 <sup>†</sup>
Subcutaneous adipose tissue (ml) <sup>α</sup>	14,671.9 (12,821.4–16,794.7)	10,335.1 (6,806.9–11,174.0)	9,613.5 (7,293.9–10,555.2)	<0.001 <sup>†</sup>
Visceral adipose tissue (ml) <sup>α</sup>	7,963.1 (5,786.8–8,813.4)	4,270.6 (3,467.2–6,514.6)	3,885.8 (2,218.2–4,566.0)	<0.001 <sup>†</sup>
BAT volume (ml) <sup>β</sup>	840.37 (602.00–1228.52)	813.86 (679.27–913.57)	690.22 (530.47–1,114.19)	0.285
BAT fat-fraction (%) <sup>β</sup>	65.62 (60.14–68.95)	65.21 (56.97–67.54)	65.55 (62.49–67.33)	0.836
BAT T2* (ms) <sup>β</sup>	11.94 (11.09–14.04)	11.20 (10.87–12.07)	11.37 (10.91–12.00)	0.500
WAT volume (ml) <sup>β</sup>	2,680.56 (2,290.51–3,542.19)	1,900.40 (948.23–2,951.76)	1,828.52 (1,186.34–2,070.82)	0.001 <sup>†</sup>
WAT fat-fraction (%) <sup>β</sup>	84.41 (82.30–85.69)	79.91 (66.27–81.66)	77.17 (71.11–80.34)	<0.001 <sup>†</sup>
WAT T2* (ms) <sup>β</sup>	59.28 (50.84–65.29)	50.21 (39.64–61.07)	48.23 (31.98–55.91)	<0.001 <sup>†</sup>

Continuous variables are expressed in median (interquartile range) for non-parametric analysis

M0 pre-op MRI, M6 6-month post-op MRI, M12 12-month post-op MRI

<sup>†</sup> Indicates at least one group of significant differences using Friedman's test and post-hoc analysis will be carried out

<sup>α</sup> Indicates measurements at the abdominal level

<sup>β</sup> Indicates measurements at the interscapular, supraclavicular and cervical regions

Proton MR spectroscopy with STEAM sequence (TE = 15 ms, TR = 5,000 ms, NSA = 24, data points = 2,048, spectral width = 2,000 Hz) was performed in the same scan with the torso coil to acquire a spectrum of IHTG. A 30 x 30 x 30 mm<sup>3</sup> voxel was placed in the right liver lobe (e.g. Couinaud segment V–VIII). A survey was performed to help in positioning the voxel and avoiding major vessels. Short TE and long TR were selected to minimize T2 and T1 effects. Non-breath-hold scan was performed and the acquisition time was approximately 2 min. Data were exported for offline spectral analysis.

### Measurement of brown and white adipose tissues

In this study, BAT was segmented and measured using an algorithm based on a Gaussian mixture model in co-registered fat-fraction and T2\* images [13]. This algorithm differentiated BAT from WAT using their intrinsic properties of fat-fraction and T2\* signals [13–15]. BAT was highly specialized for non-shivering thermogenesis due to its unique characteristic of uncoupling protein 1 (UCP1). The abundance of iron-rich mitochondria with UCP 1 in brown adipocytes accelerated dephasing of transverse magnetization, which caused a lower T2\* signal from BAT, and its heat production function also reduced fat-fraction content [16]. This algorithm first extracted fat tissues in the fat-only images followed by using Gaussian mixture model and EM algorithm to cluster

different groups of voxels, e.g. BAT, WAT and background using their corresponding T2\* and fat-fraction values. Distributions with moderate fat-fraction and low T2\* are indicative of BAT while those with high fat-fraction and high T2\* favour the presence of WAT. This algorithm also measured the MR properties and volume of supraclavicular WAT in the same region of BAT. Full details are shown in the publication by Hui et al [13]. Figure 1a and b show the anatomical location and 3D rendering of BAT.

For abdominal WAT, SAT and VAT were segmented and measured using an algorithm that automatically detected and removed the narrow connecting regions between them [17]. This algorithm utilized Bresenham's Line method and Midpoint Circle method to construct a spoke-like template, and this template was applied to the scan over the adipose tissue to separate SAT and VAT. Figure 2a illustrates the anatomical locations of subcutaneous and visceral adipose tissues at the abdominal level, liver and pancreas. Figure 2b and c show 3D renderings of SAT and VAT respectively.

### Measurement of intrahepatic triglyceride (IHTG) and pancreas fat-fraction

A 1H MR spectroscopy was performed to measure IHTG. A 30 x 30 x 30 mm<sup>3</sup> (27 ml) voxel was positioned in the right liver lobe and major vessels were avoided based on the survey scan. Data were exported for spectral analysis using the

jMRUI software package [18]. Lipid peaks were measured for relative fat signal integrals in terms of a percentage of the total signal amplitude. IHTG content was calculated as  $[I_{\text{fat}}/(I_{\text{fat}} + I_{\text{water}})] \times 100$ , where  $I_{\text{fat}}$  and  $I_{\text{water}}$  represented peak amplitudes of fat and water, respectively [19]. NAFLD was defined as an IHTG content of more than the threshold of 5.56%, alcohol consumption of no more than 30 g/day for males and 20g/day for females, no known liver diseases including hepatitis B- or C-positive test, and no ingestion of medications known to produce hepatic steatosis [20–23].

Pancreatic fat-fraction and  $T2^*$  were measured using the fat-fraction images. Three operator-defined regions of interest (ROIs) were drawn on the caput, corpus and cauda of the pancreas by an experience radiologist. The area of the ROIs was set at around  $1.0 \text{ cm}^2$  for most measurements. Major blood vessels including the superior mesenteric artery and superior mesenteric vein near the caput and pancreatic duct were carefully avoided to prevent signal contamination. Signal intensities from the three ROIs were averaged as the final result.  $T2^*$  values were captured simultaneously in the co-registered  $T2^*$  images. The pancreatic measurements were performed twice independently, one by a radiologist and one by a PhD fellow with a medical degree. Results from the radiologist were used for analysis and the second measure was used to measure the inter-observer variation. Unlike NAFLD, there is no well-recognized threshold to determine the upper bound of pancreatic fat for healthy individuals. In this study, 10.4% was adopted as the upper limit for normal based on a study of 685 healthy volunteers from the general population [24].

## Data analysis

For non-parametric analysis, Friedman's test was performed to compare differences between groups for repeated measures variables acquired from three different time points, i.e. pre-op MRI (M0), 6-month post-op MRI (M6) and 12-month post-op MRI (M12) using SPSS (SPSS Statistics version 24, IBM, Armonk, NY, USA). A 2-sided  $p$ -value of  $<0.05$  was taken as statistically significant and follow-up post-hoc analyses were carried out. All continuous variables are expressed as median (interquartile range). Wilcoxon's signed-rank test with Bonferroni correction was performed for pairwise comparisons. Bonferroni-adjusted significance level was set at  $p < 0.017$  ( $0.05/3$ ). Intraclass correlation coefficient (ICC) was used to test the inter-observer variation for pancreatic fat measurements between the two observers.

## Results

Friedman's tests indicated that weight, BMI, waist circumference, pancreatic fat-fraction, IHTG, abdominal SAT and VAT, and the volume, fat-fraction and  $T2^*$  of supraclavicular WAT

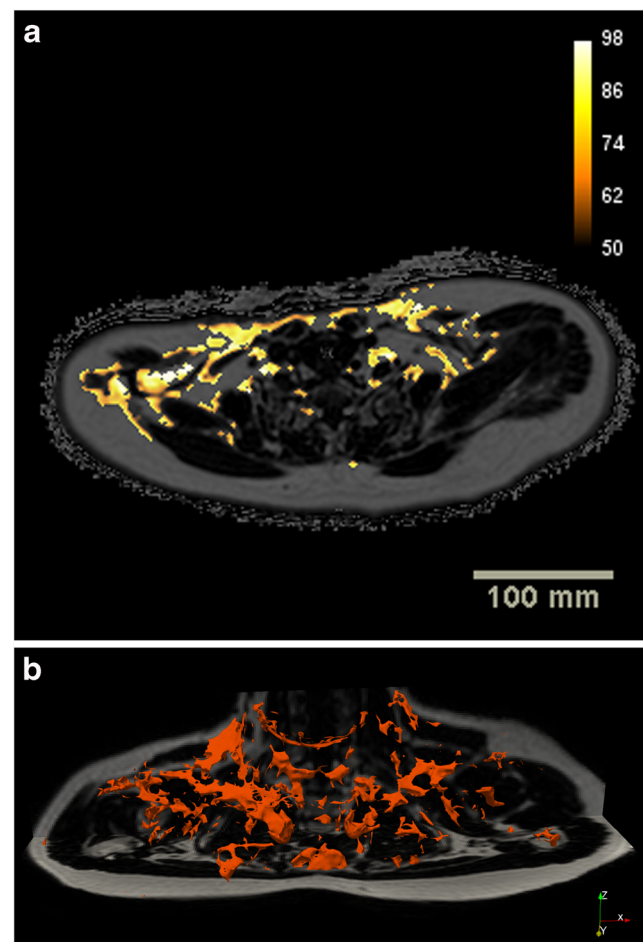


**Fig. 1** (a) Segmentation of brown adipose tissue at the level of the supraclavicular fossa and (b) 3D volumetric rendering of brown adipose tissue

were significantly different in at least one pairwise group. Full details and  $p$ -values are shown in Table 1. Nine out of 12 (75%) participants were diagnosed with NAFLD using MRS at baseline before surgery and only one remained NAFLD at M6 and all resolved by M12. Figure 3a–d show the percentage of change in IHTG content, pancreatic fat-fraction, abdominal SAT and VAT, respectively, from baseline to M6 and M12. No significant changes were observed in the volume of BAT, as shown in Fig. 3e.

Post-hoc analysis was performed using Wilcoxon's signed-rank test. Pairwise comparisons indicated significant decreases in weight ( $p=0.005$ ) and BMI ( $p=0.005$ ) among all three pair groups. For waist circumference, significant decreases were observed between M0 and M12 ( $p=0.005$ ) and M6 and M12 ( $p=0.007$ ). Body weight was reduced by 18.8% (96.1 kg to 78.0 kg) and 12.9% (78.0 kg to 67.9 kg) between baseline and M6 and M6 and M12, respectively, while waist circumference was reduced by 14.1% (105.3 cm to 90.5 cm) between M6 and M12.

For other MRI-based variables, pancreatic fat-fraction was significantly ( $p=0.009$ ) reduced by 67.3% (6.71% to 2.19%)

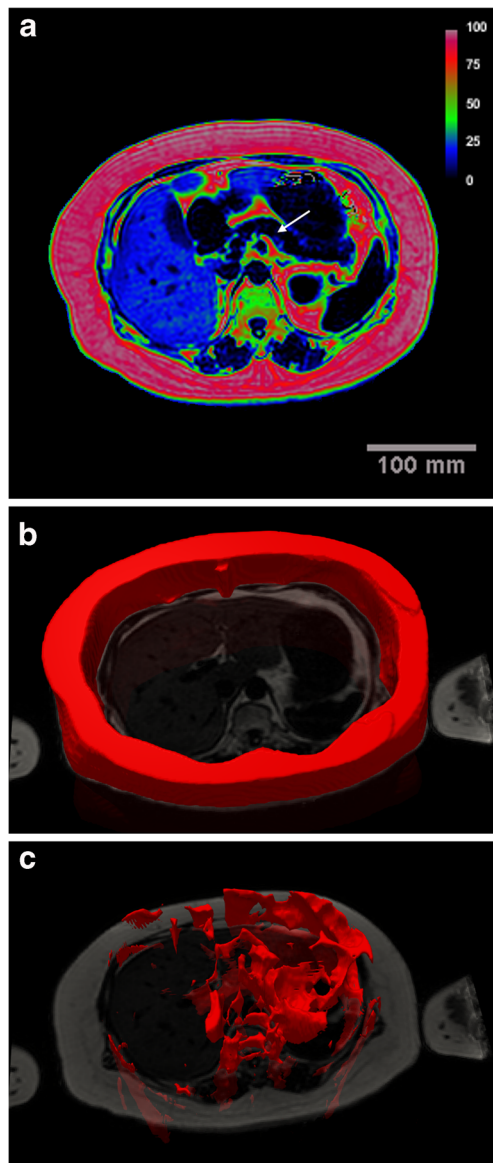


**Fig. 2** (a) Fat-fraction image showing the anatomical view of abdominal white adipose tissue (red) including subcutaneous and visceral fat, liver (blue) and pancreas (white arrow). (b) 3D volumetric renderings of subcutaneous adipose tissue and (c) visceral adipose tissue

between M0 and M12. The median was 6.71% (IQR: 4.29–10.57%) at baseline. Using 10.4% as the upper bound for normal, two out of 12 (16.7%) participants had pancreatic fat-fraction above the limit and one at a marginal level with 10.2% fat-fraction. Despite the small sample size, the rate of fatty pancreas in this study was similar to the population-based study with a prevalence of 16.1% [24]. For the rest of the variables including IHTG, abdominal SAT and VAT, and supraclavicular WAT (volume/fat-fraction/T2\*), similar patterns were observed with significant decreases between M0 and M6 and M0 and M12 (all  $p < 0.01$ ), but no differences between M6 and M12. Full details are shown in Table 2.

Inter-observer variation for pancreatic fat measurement showed good reliability as the ICC was 0.732 on average measure with absolute agreement [25].

## Discussion

This study measured the change in fat content and other major indicators of obesity in a group of volunteers before and after bariatric surgery. The volume of abdominal WAT and fat-fractions of the liver and pancreas were significantly reduced after bariatric surgery as well as weight and waist circumference. The reduction in weight and waist circumference was mostly contributed by a decrease in abdominal WAT due to the reduction of food intake and energy absorption. Food intake was reduced due to a large portion of the greater curvature being excised or restricted. Furthermore, fasting ghrelin level was believed to play a role in the stimulation of food intake and research studies reported that it was significantly suppressed in patients after bariatric surgery [26, 27], which could be an additional factor contributing to weight loss in this study. Liver fat content was reduced below the threshold in all patients with NAFLD 1 year after surgery while a similar change was observed in pancreatic fat. Fat-fraction, T2\* and volume of BAT remained unchanged, but those of WAT at the supraclavicular fat depot were significantly reduced 6 months after surgery. The composition and volume of BAT may not be affected by the surgery itself but the underlying change in BAT activity could not be ruled out.

Hepatic steatosis and non-alcoholic fatty liver disease (NAFLD) are commonly seen in obese individuals. In this study, 75% of participants were diagnosed with NAFLD at baseline. In those with NAFLD, 89% of them were resolved at 6 months and all resolved below the threshold of 5.56% 1 year after the surgery, which was in agreement with some other studies [28, 29]. A recent study also reported similar results as 84% of patients with NAFLD achieved resolution in 6 months as liver fat-fraction was reduced from 16.6% to 4.4%, which was also comparable to the results from this study [30]. Our results suggest that bariatric surgery helped to reverse the condition of NAFLD likely due to the reduction of serum free fatty acid circulating to the liver and intrahepatic fatty acids used for oxidation to provide energy, resulting in a positive correlation between free fatty acid and NAFLD [31, 32]. Three other participants (BMI 32, 33 and 38 kg/m<sup>2</sup>, respectively) showed normal IHTG at baseline. The exact mechanism for why some obese participants did not accumulate excessive liver fat remained uncertain.

For pancreatic fat-fraction, significant reduction was observed between M0 and M12, which could possibly be due to the decrease in adipocyte infiltration in pancreatic exocrine tissue due to the reduced dietary fatty acid from food intake. The reduction of pancreatic fat was also associated with improved  $\beta$ -cell function and glucose control [33]. Pancreatic T2\* was increased but not significantly from 42.92 ms to 50.86 ms between M0 and

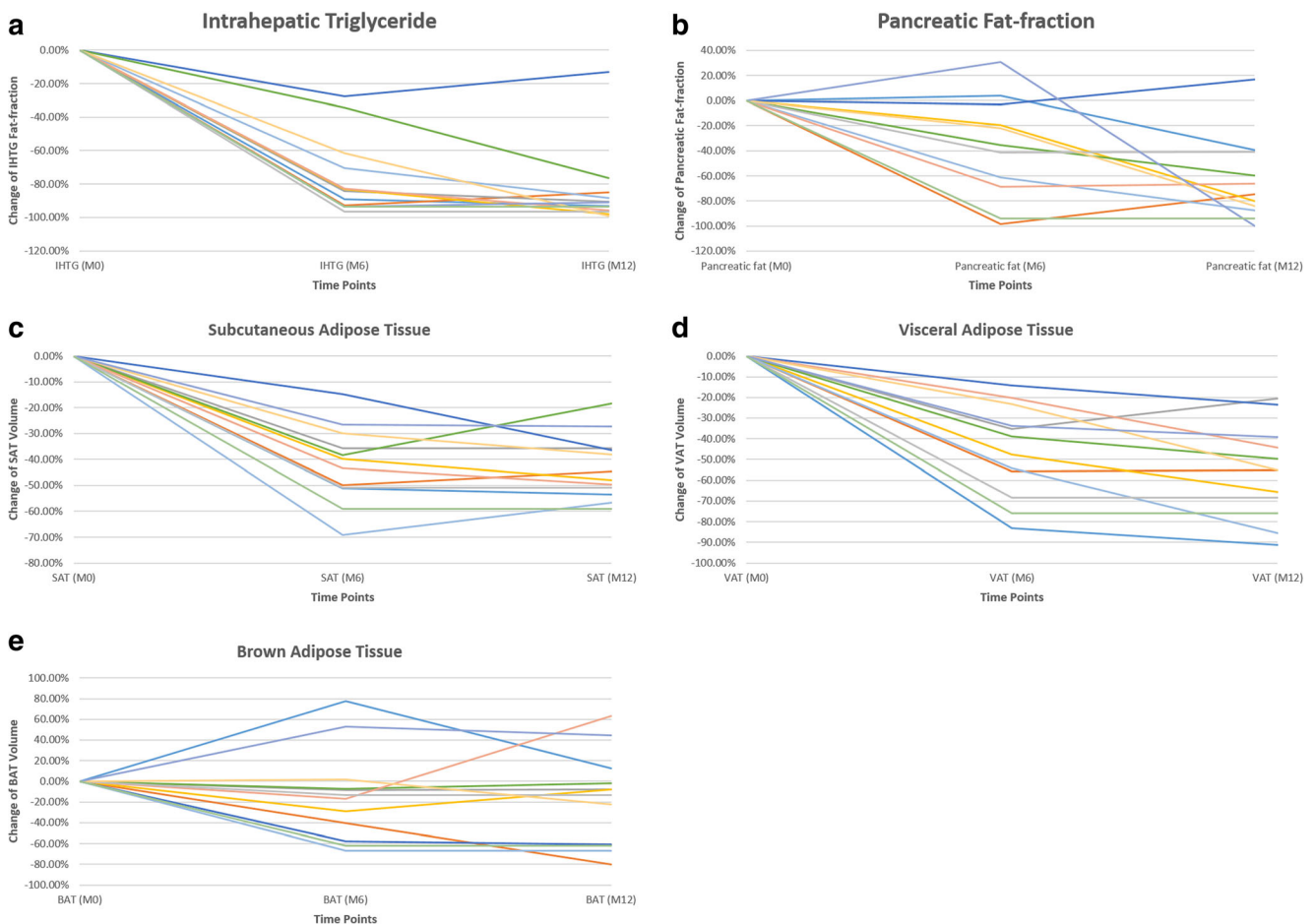


**Fig. 3** Line plots for the percentage of change from M0 to M12 of (a) intrahepatic triglyceride, (b) pancreatic fat-fraction, (c) subcutaneous adipose tissue, (d) abdominal visceral adipose tissue and (e) brown adipose tissue.

M6, and became stable thereafter. One possible explanation would be the reduction of insulin production due to the increased insulin sensitivity from the improved hyperinsulinemia state after

weight reduction and fat loss. A less active pancreas might require lower blood consumption, which led to the decrease of iron concentration detected by MRI.

**Table 2** *p*-values in the Wilcoxon signed-rank test with Bonferroni correction for post-hoc analysis

	M0	M6	M12	M0 vs. M6 <i>p</i> -value	M0 vs. M12 <i>p</i> -value	M6 vs. M12 <i>p</i> -value
Weight (kg)	96.1	78.0	67.9	0.005 <sup>†</sup>	0.005 <sup>†</sup>	0.005 <sup>†</sup>
BMI (kg/m <sup>2</sup> )	35.2	27.9	26.3	0.005 <sup>†</sup>	0.005 <sup>†</sup>	0.005 <sup>†</sup>
Waist circumference (cm)	111.0	105.3	90.5	0.066	0.005 <sup>†</sup>	0.007 <sup>†</sup>
Pancreatic fat-fraction (%)	6.71	5.05	2.19	0.114	0.009 <sup>†</sup>	0.028
Intrahepatic triglyceride (%)	14.66	2.09	0.87	0.005 <sup>†</sup>	0.005 <sup>†</sup>	0.169
Subcutaneous adipose tissue (ml) <sup>α</sup>	1,4761.9	10,335.1	9,613.5	0.005 <sup>†</sup>	0.005 <sup>†</sup>	0.441
Visceral adipose tissue (ml) <sup>α</sup>	7,963.1	4,270.6	3,885.8	0.005 <sup>†</sup>	0.005 <sup>†</sup>	0.028
WAT volume (ml) <sup>β</sup>	2,680.56	1,900.40	1,828.52	0.005 <sup>†</sup>	0.005 <sup>†</sup>	0.214
WAT fat-fraction (%) <sup>β</sup>	84.41	79.91	77.17	0.005 <sup>†</sup>	0.005 <sup>†</sup>	0.110
WAT T2* (ms) <sup>β</sup>	59.28	50.21	48.23	0.009 <sup>†</sup>	0.005 <sup>†</sup>	0.214

<sup>†</sup> Indicates significant difference with Bonferroni-adjusted level at (0.05/3) 0.017

<sup>α</sup> Indicates measurements at the abdominal level

<sup>β</sup> Indicates measurements at the interscapular, supraclavicular and cervical regions

For abdominal subcutaneous and visceral adipose tissues, significant decreases were observed between M0 and M6 but not between M6 and M12. Results indicated that SAT rapidly reduced only in the first 6 months after surgery and became stable afterward. For VAT, a strong trend ( $p=0.028$ , considered not significant in Bonferroni-adjusted significance level) of reduction continued in the second 6-month interval. VAT was considered more metabolically active as it secretes a fat-related hormone and cytokine, as internal fat caused more severe health consequences and the substantial loss of VAT inferred that VAT required a longer time to be consumed.

Another important objective of this study was to measure the change in BAT. Unlike other studies using  $^{18}\text{F}$  PET-CT, our method measured the absolute volume of BAT independent from its activation state using MRI. Our results indicated that no significant changes were observed in BAT volume as well as  $T2^*$  and fat-fraction composition before and after surgery. This observation suggested that the volume and MR properties of BAT were not affected by the change of overall adipose tissues. Small sample size and longer time required for BAT recruitment could be the underlying explanation for the observed negative changes of BAT in this cohort. Power analysis was crucial to validate the findings, as the process of BAT recruitment might occur as a slow mechanism. In addition, BAT has a physiological role in human metabolism and the activity of BAT is changed in obese individuals after surgery, as shown by the increased proportion of BAT [34–36], whereas this study measured the absolute volume of BAT independent of their activation state. This might explain why the results for BAT remained unchanged, because both active and inactive BAT were included using our proposed method.

Furthermore, we measured the change of supraclavicular WAT from the same region of BAT. Results indicated that fat-fraction and  $T2^*$  were significantly reduced between baseline and M6, and continued to reduce between M6 and M12 at a slower rate. The significant changes of these two properties indicated that the internal properties of WAT or at least part of them at that region were altered after surgery. A possible explanation would be the process of browning, which refers to the process of turning white adipose tissue into beige. Browning is a relatively new term used to describe the change of white adipocytes to thermogenic beige adipocytes by exogenous stimuli such as chronic cold exposure or endogenous factors such as treatment with  $\beta_3$ -adrenergic receptor activators, thyroid hormone and natriuretic peptides [37–39]. Beige adipocytes have similar functional characteristics of typical brown adipocytes but they have a distinct origin of gene expression [40]. In terms of their MR properties, the reduction of  $T2^*$  might be contributed to by the emergence of UCP1 cells in browning, which triggered the thermogenic function to reduce internal fat-fraction. The browning process is partially supported by the study from Vijgen et al, who concluded that recruitment of BAT in patients after LSG was possible [35].

Several limitations to this study should be taken into account. PET-CT is a more representative method for the detection of BAT. However, it is not ethical to have volunteers undergo additional procedures with high radiation exposure. MRI is an alternative approach that many concepts and theories has proposed over the last few years. However, no gold standard has been achieved yet. Furthermore, the sample size was small due to the limited number of cases undergoing bariatric surgery every year.

In conclusion, this study demonstrated that bariatric surgery effectively reduced patients' weight, waist circumference, volume of abdominal SAT and VAT, IHTG and pancreatic fat. Rapid reduction was observed in the first 6-month interval after surgery while the progress became more gentle and consistent in the second 6-month interval. Patients with NAFLD all resolved 12 months after surgery and pancreatic fat was also reduced below the threshold. No significant changes were observed in volume, fat-fraction and  $T2^*$  of BAT and those of WAT at the supraclavicular fat depot were significantly reduced.

**Acknowledgements** The authors would like to thank Candice Lam and Sabrina Ler for their kind support and assistance with subject recruitment.

**Funding** This study has received funding by the Research Grant Council of Hong Kong. The work described in this paper was partially supported by grants from the Research Grants Council (Project No.: 14206716 and SEG\_CUHK02) of the Hong Kong Special Administrative Region

## Compliance with ethical standards

**Guarantor** The scientific guarantor of this publication is Winnie CW Chu.

**Conflict of interest** The authors of this paper declare no relationships with any companies whose products or services may be related to the subject matter of the article.

**Statistics and biometry** No complex statistical methods were necessary for this paper.

**Informed consent** Written informed consent was obtained from all subjects (patients) in this study.

**Ethical approval** Institutional Review Board approval was obtained.

## Methodology

- prospective
- longitudinal study
- performed at one institution

## References

1. McFarlane SI, Banerji M, Sowers JR (2001) Insulin resistance and cardiovascular disease. *J Clin Endocrinol Metab* 86:713–718

2. Kawano Y, Cohen DE (2013) Mechanisms of hepatic triglyceride accumulation in non-alcoholic fatty liver disease. *J Gastroenterol* 48:434–441
3. Enerbäck S (2010) Brown adipose tissue in humans. *Int J Obes (Lond)* 34(Suppl 1):S43–S46
4. Cypess AM, Lehman S, Williams G et al (2009) Identification and importance of brown adipose tissue in adult humans. *N Engl J Med* 360:1509–1517
5. van Marken Lichtenbelt WD, Vanhomerig JW, Smulders NM et al (2009) Cold-activated brown adipose tissue in healthy men. *N Engl J Med* 360:1500–1508
6. Ricquier D (2011) Uncoupling protein 1 of brown adipocytes, the only uncoupler: a historical perspective. *Front Endocrinol (Lausanne)* 2:85
7. Goodpaster BH, Delany JP, Otto AD et al (2010) Effects of diet and physical activity interventions on weight loss and cardiometabolic risk factors in severely obese adults: a randomized trial. *JAMA* 304:1795–1802
8. Unick JL, Beavers D, Jakicic JM et al (2011) Effectiveness of lifestyle interventions for individuals with severe obesity and type 2 diabetes: results from the Look AHEAD trial. *Diabetes Care* 34:2152–2157
9. Wadden TA, Webb VL, Moran CH, Bailer BA (2012) Lifestyle modification for obesity: new developments in diet, physical activity, and behavior therapy. *Circulation* 125:1157–1170
10. Karlsson J, Taft C, Rydén A, Sjöström L, Sullivan M (2007) Ten-year trends in health-related quality of life after surgical and conventional treatment for severe obesity: the SOS intervention study. *Int J Obes (Lond)* 31:1248–1261
11. Liu SY, Wong SK, Lam CC, Yung MY, Kong AP, Ng EK (2015) Long-term Results on Weight Loss and Diabetes Remission after Laparoscopic Sleeve Gastrectomy for A Morbidly Obese Chinese Population. *Obes Surg* 25:1901–1908
12. Karmali S, Schauer P, Birch D, Sharma AM, Sherman V (2010) Laparoscopic sleeve gastrectomy: an innovative new tool in the battle against the obesity epidemic in Canada. *Can J Surg* 53:126–132
13. Hui SCN, Ko JKL, Zhang T et al (2017) Quantification of brown and white adipose tissue based on Gaussian mixture model using water-fat and T2\* MRI in adolescents. *J Magn Reson Imaging* 46:758–768
14. Hu HH, Perkins TG, Chia JM, Gilsanz V (2013) Characterization of human brown adipose tissue by chemical-shift water-fat MRI. *AJR Am J Roentgenol* 200:177–183
15. Hu HH, Smith DL Jr, Nayak KS, Goran MI, Nagy TR (2010) Identification of brown adipose tissue in mice with fat-water IDEAL-MRI. *J Magn Reson Imaging* 31:1195–1202
16. Koskensalo K, Raiko J, Saari T et al (2017) Human Brown Adipose Tissue Temperature and Fat Fraction Are Related to Its Metabolic Activity. *J Clin Endocrinol Metab* 102:1200–1207
17. Hui SCN, Zhang T, Shi L, Wang D, Ip CB, Chu WCW (2017) Automated segmentation of abdominal subcutaneous adipose tissue and visceral adipose tissue in obese adolescent in MRI. *Magn Reson Imaging* 45:97–104
18. Stefan D, Cesare FD, Andrasescu A et al (2009) Quantitation of magnetic resonance spectroscopy signals: the jMRUI software package. *Meas Sci Technol* 20:104035–104044
19. van Werven JR, Hoogduin JM, Nederveen AJ et al (2009) Reproducibility of 3.0 Tesla magnetic resonance spectroscopy for measuring hepatic fat content. *J Magn Reson Imaging* 30:444–448
20. Szczepaniak LS, Nurenberg P, Leonard D et al (2005) Magnetic resonance spectroscopy to measure hepatic triglyceride content: prevalence of hepatic steatosis in the general population. *Am J Physiol Endocrinol Metab* 288:E462–E468
21. Fabbrini E, Sullivan S, Klein S (2010) Obesity and nonalcoholic fatty liver disease: biochemical, metabolic, and clinical implications. *Hepatology* 51:679–689
22. Chalasani N, Younossi Z, Lavine JE et al (2012) The diagnosis and management of non-alcoholic fatty liver disease: practice Guideline by the American Association for the Study of Liver Diseases, American College of Gastroenterology, and the American Gastroenterological Association. *Hepatology* 55:2005–2023
23. European Association for the Study of the Liver (EASL), European Association for the Study of Diabetes (EASD) & European Association for the Study of Obesity (EASO) (2016) EASL-EASD-EASO Clinical Practice Guidelines for the management of non-alcoholic fatty liver disease. *Diabetologia* 59(6):1121–1140
24. Wong VW, Wong GL, Yeung DK et al (2014) Fatty pancreas, insulin resistance, and beta-cell function: a population study using fat-water magnetic resonance imaging. *Am J Gastroenterol* 109:589–597
25. Cicchetti DV (1994) Guidelines, Criteria, and Rules of Thumb for Evaluating Normed and Standardized Assessment Instruments in Psychology. *Psychological Assessment* 6:284–290
26. Karamanakos SN, Vagenas K, Kalfarentzos F, Alexandrides TK (2008) Weight loss, appetite suppression, and changes in fasting and postprandial ghrelin and peptide-YY levels after Roux-en-Y gastric bypass and sleeve gastrectomy: a prospective, double blind study. *Ann Surg* 247:401–407
27. Cummings DE, Weigle DS, Frayo RS et al (2002) Plasma ghrelin levels after diet-induced weight loss or gastric bypass surgery. *N Engl J Med* 346:1623–1630
28. Taitano AA, Markow M, Finan JE, Wheeler DE, Gonzalvo JP, Murr MM (2015) Bariatric surgery improves histological features of nonalcoholic fatty liver disease and liver fibrosis. *J Gastrointest Surg* 19:429–437
29. Bower G, Toma T, Harling L et al (2015) Bariatric Surgery and Non-Alcoholic Fatty Liver Disease: a systematic review of liver biochemistry and histology. *Obes Surg* 25:2280–2289
30. Luo RB, Suzuki T, Hooker JC et al (2018) How bariatric surgery affects liver volume and fat density in NAFLD patients. *Surg Endosc* 32:1675–1682
31. Immonen H, Hannukainen JC, Kudomi N et al (2018) Increased Liver Fatty Acid Uptake Is Partly Reversed and Liver Fat Content Normalized After Bariatric Surgery. *Diabetes Care* 41:368–371
32. Zhang J, Zhao Y, Xu C et al (2014) Association between serum free fatty acid levels and nonalcoholic fatty liver disease: a cross-sectional study. *Sci Rep* 4:5832
33. Honka H, Koffert J, Hannukainen JC et al (2015) The effects of bariatric surgery on pancreatic lipid metabolism and blood flow. *J Clin Endocrinol Metab* 100:2015–2023
34. Vijgen GH, Bouvy ND, Teule GJ, Brans B, Schrauwen P, van Marken Lichtenbelt WD (2011) Brown adipose tissue in morbidly obese subjects. *PLoS One* 6:e17247
35. Vijgen GH, Bouvy ND, Teule GJ et al (2012) Increase in brown adipose tissue activity after weight loss in morbidly obese subjects. *J Clin Endocrinol Metab* 97:E1229–E1233
36. Dadson P, Hannukainen JC, Din MU et al (2018) Brown adipose tissue lipid metabolism in morbid obesity: Effect of bariatric surgery-induced weight loss. *Diabetes Obes Metab*. <https://doi.org/10.1111/dom.13233>
37. Wu J, Boström P, Sparks LM et al (2012) Beige adipocytes are a distinct type of thermogenic fat cell in mouse and human. *Cell* 150:366–376
38. Martínez-Sánchez N, Moreno-Navarrete JM, Contreras C et al (2017) Thyroid hormones induce browning of white fat. *J Endocrinol* 232:351–362
39. Sampath SC, Bredella MA, Cypess AM, Torriani M (2016) Imaging of Brown Adipose Tissue: State of the Art. *Radiology* 280:4–19
40. Bartelt A, Heeren J (2014) Adipose tissue browning and metabolic health. *Nat Rev Endocrinol* 10:24–36